THE

PHYSICAL REVIEW

A journal of experimental and theoretical physics established by E. L. Nichols in 1893

SECOND SERIES, VOL. 110, NO. 6 — JUNE 15, 1958

X-Rays from Visible Aurorae at Minneapolis*

J. R. WINCKLER, L. PETERSON, R. ARNOLDY, AND R. HOFFMAN
University of Minnesota, Minneapolis, Minnesota
(Received February 5, 1958)

During three auroral storms on June 30–July 1, September 12–13, and September 22–23, 1957, we have observed bursts of x-rays during balloon flights at 10 g/cm^2 depth in the atmosphere over Minneapolis. The x-rays have an energy of from 50 to 100 kev, an integrated intensity from 0.03 to 0.14 mr, and a maximum measured peak intensity of 0.4 mr/hr. One burst was observed at 47 g/cm^2 atmospheric depth (70 000 ft), and we estimate that above the atmosphere this may have corresponded to 500 mr/hr for at least 10 minutes. The current of high-energy electrons is at least 3×10^6 electrons/cm^2 sec, and probably an order of magnitude greater, and is therefore approximately equal to auroral proton fluxes, and to the fluxes observed in soft radiation at rocket heights. The x-ray bursts usually appear when a homogeneous auroral arc develops a strong ray structure, or when rays increase in intensity. The inferred energy and high velocity of the primary auroral electrons necessitates an acceleration mechanism near the earth to avoid contradictions with the commonly accepted sun-earth transit times for corpuscular beams.

I. INTRODUCTION

IN a recent Letter[1] we described a series of increases in the rates of cosmic-ray detectors flown on a balloon during an auroral storm on June 30–July 1, 1957, at Minneapolis. Following this chance measurement, we have anticipated two further auroral storms and obtained similar increases at high altitude. On the latter of these a shielded counter selective to photons gave conclusive evidence that the phenomenon is due to x-rays. This paper will describe the three measurements in detail and examine the energy, the intensity, the source, and the time correlation of the x-rays. The specifically cosmic-ray phenomena observed during the International Geophysical Year (IGY) flight series will be described separately. The known relation between Forbush type cosmic-ray decreases and magnetic storms indicates that the solar corpuscular stream affects cosmic rays as well as producing various terrestrial effects, and in fact we have observed cosmic-ray changes during one of the storms described here.

II. DESCRIPTION OF INSTRUMENTS

The standard IGY flight train carries a single Geiger counter with scalar, an integrating ion chamber, and a nuclear emulsion pellicle. One of the flights referred to below (IGY-18) carried in addition a shielded Geiger counter selective to photons. Balloon trajectories are obtained by photographing the ground with a 35-mm time lapse camera, which also records the cosmic-ray data and pressure. The instrumental data was telemetered for part of each balloon flight (5–6 hours), and the entire flight (up to 24 hours) was recorded by one component of the flight train. The instruments were carried on $\frac{3}{4}$-mil polyethylene balloons[2] of 135 000 cubic feet volume, and in most cases constant level performance was obtained at approximately 10 g/cm^2 atmospheric depth. A detailed description of the flight instrumentation will be given elsewhere.

The counter has a projected area of approximately 20 cm^2, which is constant with direction to within 5%. Its response is thus essentially isotropic. The operating voltage is 1000, and the filling 10 cm argon with alcohol quenching vapor. The counter operates from a transistorized high-voltage supply and is equipped with a transistorized scale of 512. Construction is of brass.

Figure 1 gives the dimensions of the three types of instruments used for these measurements. The photon counter is of 1-in. diameter copper wall and 8 in. in length. It is shielded by a group of six similar counters in anticoincidence. It has an omnidirectional projected

* This research sponsored by the U. S. National Committee for the International Geophysical Year through the National Science Foundation. Program assisted by the Office of Naval Research.

[1] J. R. Winckler and L. Peterson, Phys. Rev. **108**, 903 (1957).

[2] Manufactured by Raven Industries, Sioux Falls, South Dakota, and Winzen Research, Minneapolis.

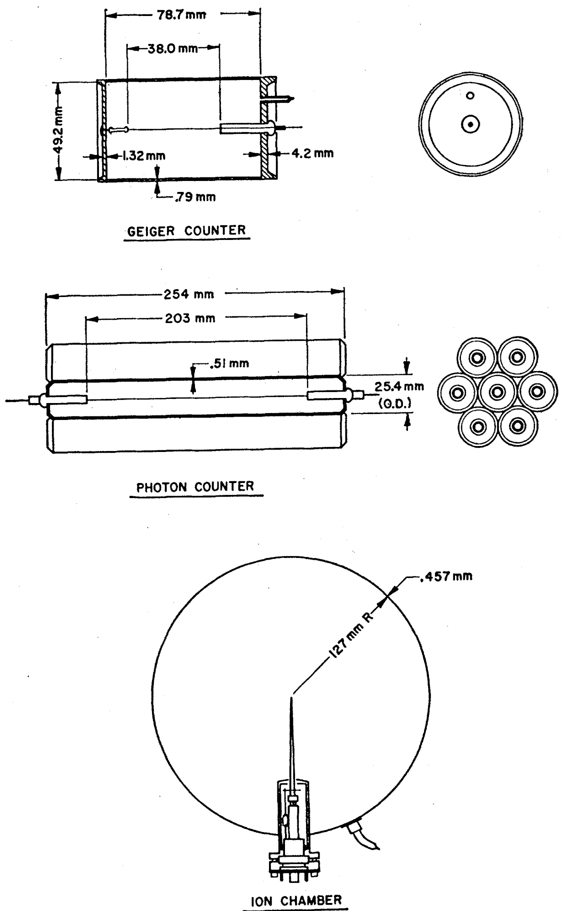

FIG. 1. Details of detecting instruments: Upper—Geiger counter (brass wall). The dimensions produce an approximately uniform omnidirectional response. Center—shielded Geiger counter (copper wall). The charged-particle leakage solid angle is computed to be not more than 1% of the total solid angle. The effective wall thickness of the detector (center counter) is 3.5 mm on the average. Bottom—steel-walled ion chamber, containing argon at 7.8 atmospheres.

area of 41.5 cm^2 on the basis of isotropic radiation, and is flown with axis horizontal. The theoretical particle leakage is less than 1% of the unshielded counting rate. Because of the extra wall thickness of the shield counters, the x-ray threshold of this counter is higher than the single Geiger unit. If the counting rate is compared with the single counter for various photon energies, the ratio (single counter)/(photon counter) decreases rapidly from ∞ at 45 kev to 1.2 at 1.2 Mev. The cutoff of the photon counter is due to the shielding effects of the surrounding counters, which increase the effective wall thickness from 0.5 mm of copper to 3 mm of copper. The photon counter is also completely transistorized, and includes a scale of 256.

The ion chamber is very similar to that used by Neher and Millikan,[3] and utilizes the Zeleny pulsing electrometer. The chamber is filled with pure argon at approximately 8 atmospheres pressure. The absolute ion current is determined by measuring the collected charge for each pulse, and since experiments show that recombination effects are negligible for γ rays, the net rate of ion production in the argon is known. The chamber calibrations are: Chamber No. 13, Flight IGY-3, 3.52×10^{-10} coulomb/pulse; Chamber No. 16, Flight IGY-18, 2.03×10^{-10} coulomb/pulse.

The ion chamber response to x-rays and γ rays has been measured and compared with the single counter. The ratio ionization/count is sensitive to the x-ray energy in the region below several hundred kilovolts.

The measured responses of the ion chamber, single counter, and photon counter are plotted in Fig. 2, for various energies of photons. These calibrations are at present rather crude. A general purpose lab ac x-ray machine was available with a range up to about 60 kev (peak ac). The ions/count ratio and the counts/photon count ratio were determined with this machine (curves A and B, respectively, in Fig. 2) and with a Co^{60} source. The cosmic-ray ions/count ratio was determined directly from flight data with the same instruments. The cosmic-ray counts/photon count ratio is computed from the geometry factors of the counter used in the two instruments, and is not at present known with very high accuracy, which probably accounts for the disagreement between curves A and B, Fig. 2, at high energy. An attempt was made to fill in the ions/count ratio in the region between 100 and 400 kev using a medical x-ray machine (Curve A', Fig. 2), but the result lies considerably higher, probably due to a great deal of soft scattered x-rays in the hospital room.

III. RESULTS

A. General Features

A typical quiet day flight is shown in Fig. 3, in which is plotted ion rate and counting rate *vs* time, for IGY-6, August 1, 1957. This flight is typical of the low cosmic-ray intensity existing during the summer of 1957 at Minneapolis, accompanying maximum of solar activity.[4] No detectable changes in rate occurred after the balloon reached ceiling altitude at 1230 U.T. The balloon remained at essentially constant altitude and geomagnetic latitude during the flight. The atmospheric cosmic-ray transition effects characteristic of omnidirectional detectors are evident as maxima in both curves at about 50 g/cm^2. The weak maximum in the ion chamber curve has appeared since the general decrease in cosmic-ray intensity referred to above[4] and reflects the relatively higher depletion of the low-energy portion of the primary spectrum.

The three cases in which increases due to auroral x-rays were observed are shown in Figs. 4, 5, and 6. Figure 4 is the July 1 occasion reported previously,[1] but an additional portion of the flight is shown with a

[3] H. V. Neher, Rev. Sci. Instr. 24, 99 (1953).

[4] J. R. Winckler and L. Peterson, Nature (to be published).

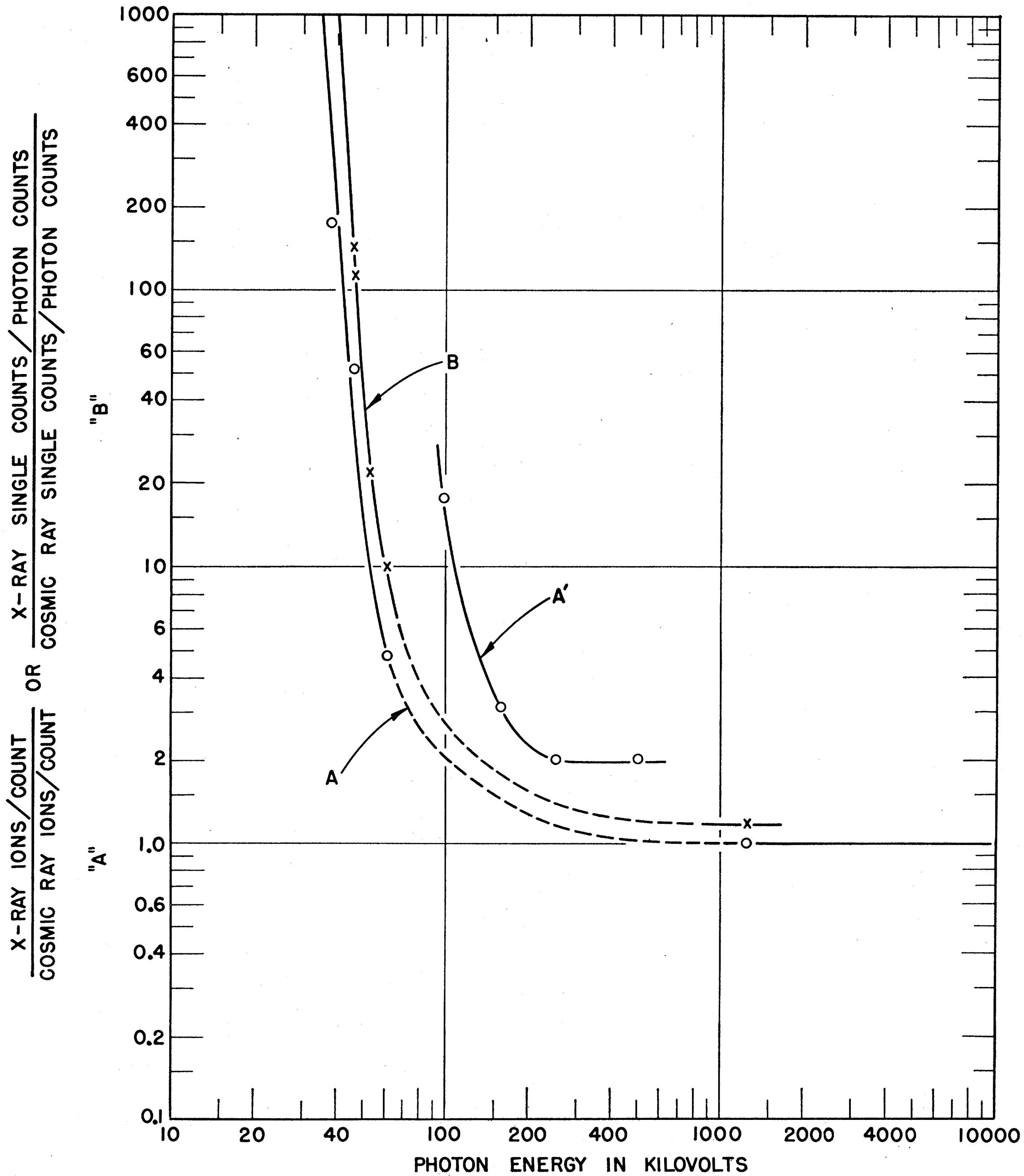

FIG. 2. Relative response of the detecting instruments to photons of various energies. Curve A, ratio (ion-chamber response)/(single-counter response) for photons, normalized to fast cosmic rays in the atmosphere. Curve B, ratio (single-counter response)/(shielded-counter response) for photons, also normalized to fast cosmic rays. Curve A', same instruments as A, but using a higher-energy x-ray machine under conditions where scattered radiation probably was important. The points at 1.2 Mev are Co^{60} γ rays.

small disturbance at 0645 U.T. The cosmic-ray features of this flight (IGY-3) are very similar to IGY-6 shown in Fig. 3. The ratio, ions/count, is plotted above Fig. 4. This ratio remains constant throughout most of the atmosphere, and increases slowly below 50 g/cm^2 atmospheric depth (after 0240 U.T.). This increase is interpreted as the effects of heavy primaries at small depths. An increase in the fluctuation of the collecting time per pulse of the ion chamber is always observed at high altitude, which may also be attributed to the increase of single events of high ionization in the chamber, such as heavy primaries. These data are uncorrected for instrument calibration factors, and differences in plotted rates between flights are not

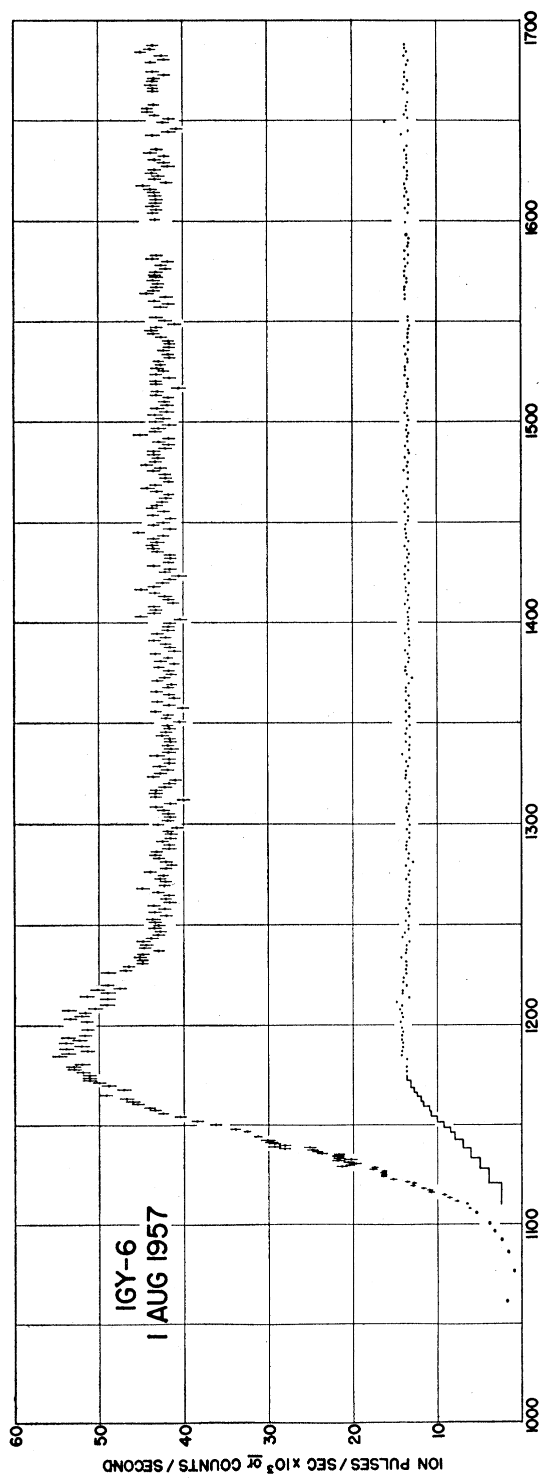

FIG. 3. A typical quiet-day flight. Upper curve—single counter. Lower curve—ion chamber. The pressure-time curve for this flight is very similar to IGY-18 (Fig. 7). The balloon reached level flight at 1230 U.T.

indicative of cosmic-ray changes. In Fig. 4 the x-ray bursts began at 0330 U.T. (2130 CST), just two minutes after the balloon reached its level ceiling of 9.6 g/cm^2 (see Fig. 7). This initial burst, No. 1 on the curve, has some structure and is followed by a subsidiary peak, No. 2. Peak No. 3 seems to be distinct, followed by a much weaker maxima, No. 4, and a later burst, beginning at 0640, after a long quiet period.

The "auroral commencement" referred to in our earlier Letter[1] is time-coincident with the start of Peak No. 1 and has been identified as the development of a homogeneous arc into strong rays, extending to the zenith. Peaks No. 2 and 3 were correlated with marked increases in visible light intensity in the ray structure. The various peaks show most clearly on the ion chamber, but are faithfully followed by the counter when intense enough to be above the counting statistical fluctuations.

Following this initial measurement on July 1, an effort was made to forecast auroral storms sufficiently in advance so that preparations for the balloon launching could be made. We are indebted to Professor Jacques Blamont of the University of Paris for calling our attention to a paper by Denisse *et al.*[5] establishing a correlation between the solar meridian passage of active sunspot regions emitting strong radio noise in the 150-Mc/sec region and the appearance of magnetic storms and associated auroras, following a time delay, for the sun-earth passage of the solar corpuscular stream, of 20 to 48 hours. Solar data for forecast purposes was obtained from the High Altitude Observatory of the University of Colorado and we are indebted to Dr. Walter Roberts and Miss Dorothy Trotter for frequent meridian passage forecasts. The daily "WASHAGI" teletype from the IGY warning center at Ft. Belvoir, Virginia, instituted during the IGY period, containing extensive solar and terrestrial data, has also been of invaluable assistance.

Another measurement, IGY-15, was successfully made on September 12–13, 1957, during a strong aurora, and the result is shown in Fig. 5. Unfortunately, owing to the necessity of reducing the flight weight to conform to CAA regulations for balloon flights during overcast conditions, only the Geiger counter unit was flown. A strong burst, Peak No. 1, was observed beginning at 0247 U.T. September 13, when the balloon had reached an atmospheric depth of 47 g/cm^2 or 70 000 ft of altitude. Some visual notes are indicated on Fig. 5, made by E. P. Ney from northern Iowa, and by observers at Minneapolis following the clearing of the overcast. This aurora was characterized by strong red color. The homogeneous arc developed into rays at about the time of the x-ray appearance. Some smaller bursts, numbered 2, 3, and 4, were observed at 8 g/cm^2 depth. For peaks 3 and 4 no observations were made of specific auroral features, and the general activity was

[5] Denisse, Steinberg, and Zisler, Compt. rend. **232**, 2290 (1951).

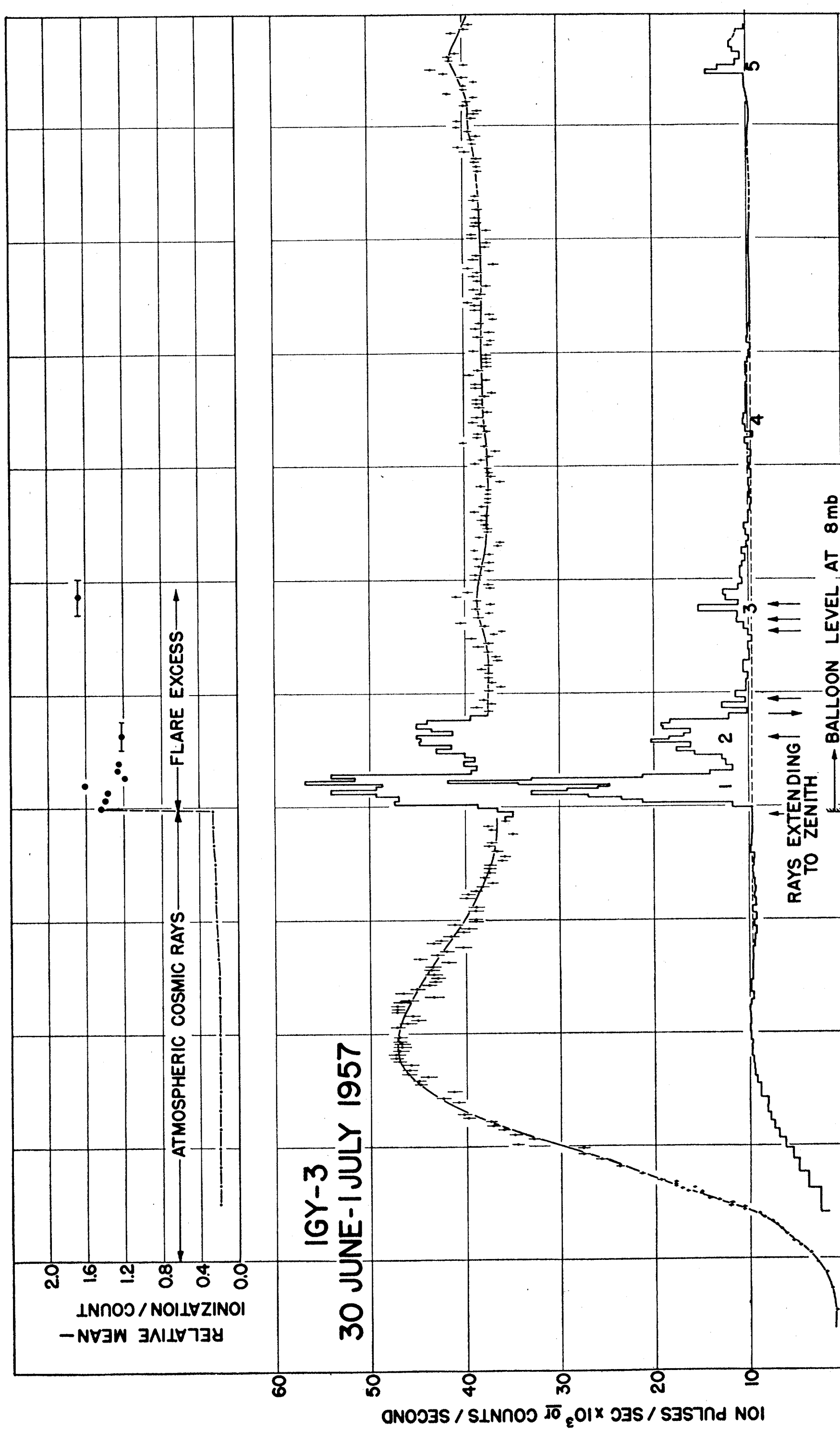

FIG. 4. Record of auroral x-rays obtained on July 1, 1957. The first burst occurred at 0330 U.T., coincident with the development of a strong ray structure and a corona. Disturbances continued until 0645 U.T. Many more hours of data are available from this flight but no further bursts were observed. The top curve shows the great difference between the bursts and normal cosmic rays in terms of the ratio (ion-chamber response)/(counter response), which is a measure of the mean dE/dx for particles, or of x-ray energy.

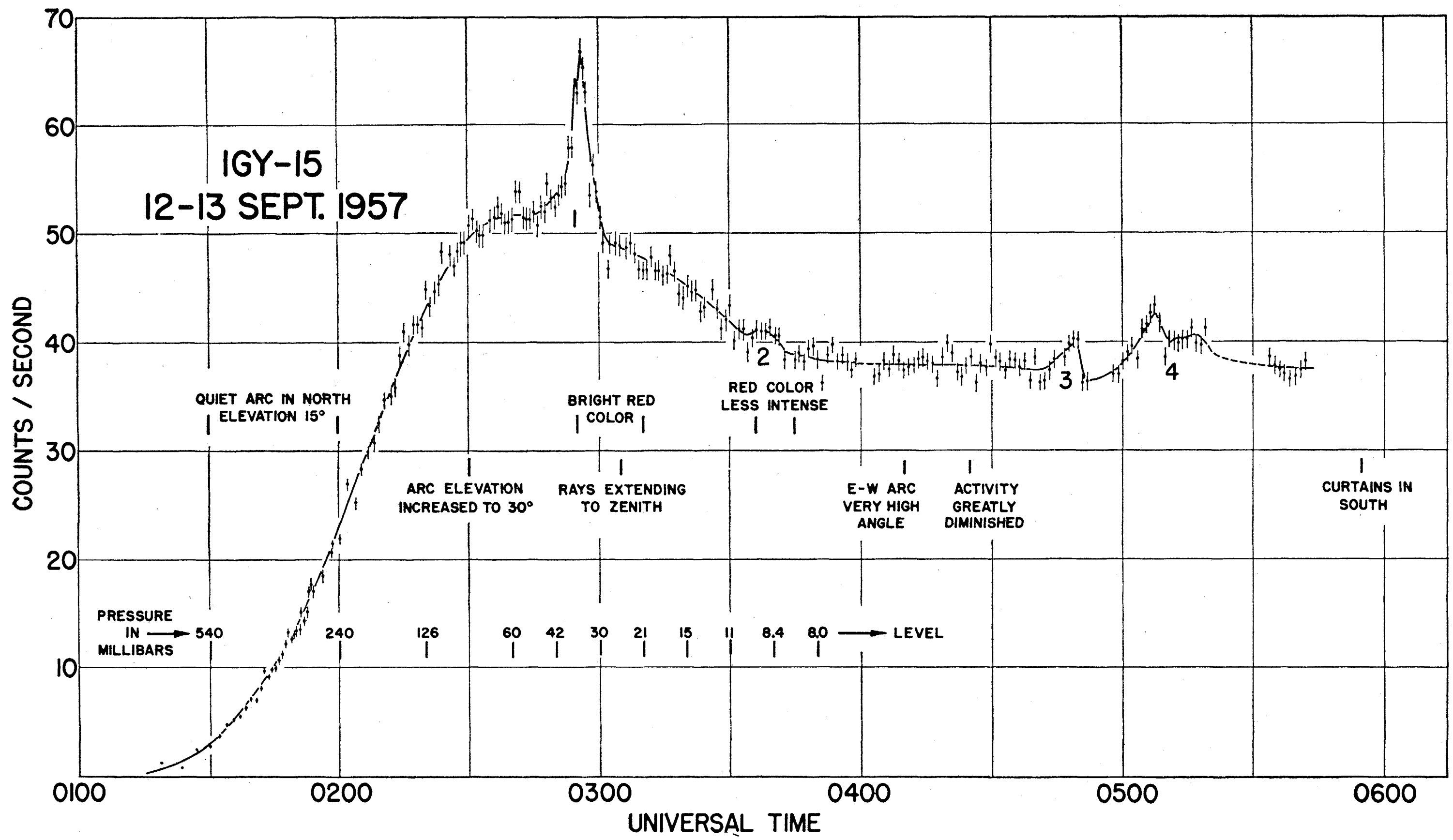

FIG. 5. Single counter record of an x-ray burst at very low level. The burst is first detectable at approximately 47 millibars, or 70 000 ft altitude, at approximately the time that ray structure appeared reaching the zenith as a corona. Strong excitation of the characteristic auroral red lines was also observed at the time of the burst.

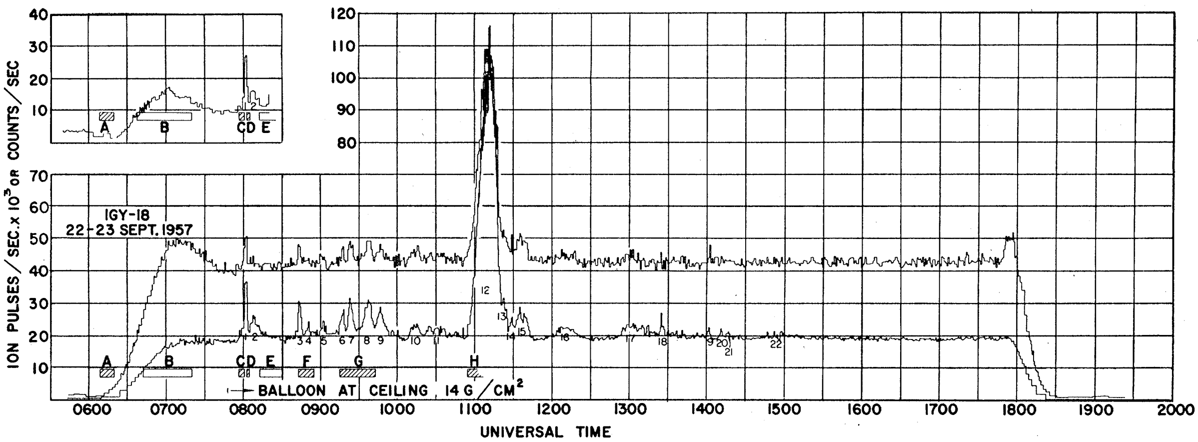

FIG. 6. Ion chamber (bottom), single counter (top), and photon counter (upper left, separate curve) response during the intense auroral storm of September 22–23, 1957. The balloon was launched about midnight C.S.T. during a lull in auroral activity, which had been very high in the earlier evening. For tabulated values of the bursts corresponding to the numbers, see Table I. The letters refer to observed auroral phenomena as follows: *A*—Flaming auroral rays reaching zenith from all points of compass. Red color. *B*—Curtains in north but activity generally decreasing overhead. (*B-C*) (0735 U.T.)—Arcs extending in narrow bands across zenith and extending almost to horizon in east and west directions. North dark. No rays. *C*—Extremely strong ray buildup from all directions. Intense red patches at 30° elevation in west. *D*—Red patches intense again after decrease. *E*—Flaming rays. No red. Activity decreased. *F*—Strong rays in northwest. Red color. Strong flaming in west. General activity increasing. *G*—Major ray buildup in west, north, and east, with corona. Red color reappeared at 0945 U.T. Following *G*, general intensity decreased with flaming rays. *H*—Very strong ray structure at 30° elevation in east with intense red color. Visible against predawn sky light.

greatly lowered. The cosmic-ray behavior during this flight closely resembles the previous cases.

The third observation was made near the end of the intense storm of September 21–22 and September 22–23, following the solar meridian passage of a very large active region on September 18–19–20. A balloon launching (IGY-17-b) was made the evening of September 21, but was unsuccessful. Besides the counter, ion chamber, and nuclear emulsions, the shielded counter selective for photons was included (see Sec. II). The equipment on IGY-17-b functioned at tree-top level throughout the night, but no x-ray effects were observed although a brilliant auroral storm continued throughout the night and was still visible at dawn. The apparatus was successfully flown again the next evening (IGY-18) with the result shown in Fig. 6. The balloon reached level flight of 14 g/cm^2 at 0750 U.T. At 0755 U.T. the first burst of x-rays occurred. In this flight the x-ray activity continued until 0300 U.T., or 0900 CST, well into the following morning. The lettered blocks under the curves represent intervals of rapidly increasing activity (cross-hatched), mostly in the form of rays, or of decreasing activity (open blocks). (See caption for Fig. 6.) In the intermediate region between blocks, activity was present in varied forms. For example, at 0735 U.T. a large arc extended from horizon to horizon across the zenith in the E-W direction. At this time the northern sky down to the horizon was quite dark. This arc apparently did not produce x-ray bursts. The x-rays began again with additional strong ray buildup at *C* and *D*.

The photon counter rate is plotted in the upper graph in Fig. 6. This instrument failed at 0830 U.T. due to improper thermalizing, but the data up to that time are considered reliable. The relative rate of increase at 0800 U.T. of this instrument above its own cosmic-ray background is approximately 3:1, or larger by a factor of 15 than the same ratio for the unshielded counter. We consider this as proof that the phenomenon measured involved x-ray photons and not particles. If the effect involved particles, the factor should be much smaller than unity, as the particle response of the shielded counter is negligible and the observed rate at high altitude is due to cosmic-ray-produced γ rays. (See Sec. II.)

The largest burst occurred at 1100 U.T., and was associated with a major ray build-up with intense red color in the Eastern sector. This giant burst may be of the type observed at much lower altitude on September 12–13. (See Fig. 3.) The large burst is followed by four successively weaker peaks, the last one at 1500 U.T. The x-ray peaks seem to build up and decrease, with much fine structure, but with a general period of about 45 minutes. This periodicity may be a characteristic time constant of the auroral phenomenon. There is evidence for this periodicity also in Fig. 4.

Nuclear emulsions flown on this flight showed definite evidence of x-ray exposure, with δ rays much more numerous on one face of the vertical stack than the other. This probably indicates a localized source of the x-rays and will be reported later by E. P. Ney *et al.*

B. Detailed Analysis

We have measured the peak and integrated intensity of each numbered burst in Figs. 4, 5, and 6 for the ion chamber and counter above cosmic-ray background,

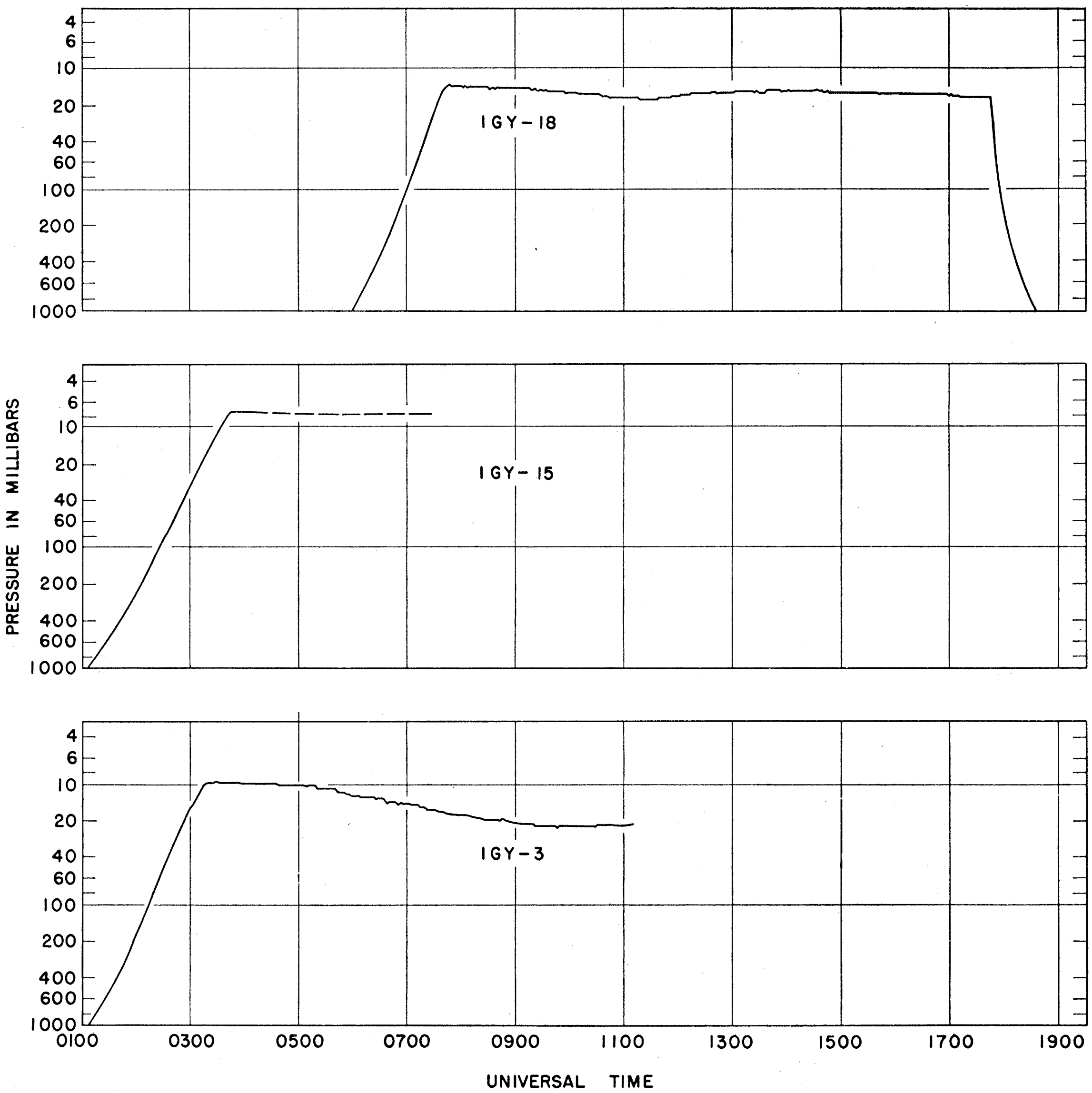

FIG. 7. Pressure-time history of the three auroral flights during periods of interest.

and these are tabulated in Table I. The integrated intensity is simply the number of ion chamber pulses or the number of Geiger counter impulses generated by the x-ray photons alone. The peak intensity is expressed in terms of counting rates above background. The ratio of ions/count for integrated and peak intensity is a function of x-ray energy or mean particle ionization as discussed in Part I, but varies from flight to flight with the particular instruments used. The last two columns tabulate the integrated and peak intensity ratios normalized to the ratio for minimum-ionizing cosmic-ray particles observed during the ascending portion of the flight.

There is a great variability in the size of the bursts, and for the smaller bursts the counter statistical fluctuations are relatively large. The final comparison with cosmic rays, however, shows that the individual bursts in one storm do not differ greatly in energy. IGY-15 on September 12 had only the counter so that energies could not be estimated.

Table II summarizes certain quantitative properties of the observations. In column 7 the weighted mean (W.M.) is obtained according to the relation W.M. = ion chamber pulses/counter pulses. The summation is above cosmic-ray background for the entire flight. From W.M./cosmic-ray ratio we infer the average x-ray energy. From the data in Table II we proceed to examine several features of the x-rays as follows:

1. Source.—We must attribute the x-rays to the bremsstrahlung of electrons in the high atmosphere

TABLE I. Analysis of x-ray bursts.

Flight No.	Burst No.	Integrated intensity Ion pulses	Integrated intensity Counts	Peak intensity Ion pulses/sec	Peak intensity Counts/sec	Ratio: ion pulses/count Integrated	Ratio: ion pulses/count Peak	X-ray ratio / Cosmic-ray ratio Integrated	X-ray ratio / Cosmic-ray ratio Peak
IGY-3	1	8.40	0.750×10^4	32.4×10^{-3}	19.8	1.12×10^{-3}	1.64×10^{-3}	5.4	7.9
	2	5.57	0.410×10^4	10.4×10^{-3}	8.0	1.36×10^{-3}	1.30×10^{-3}	6.5	6.3
	3	2.56	0.079×10^4	5.6×10^{-3}	3.2	3.3×10^{-3}	1.75×10^{-3}	15.9	8.4
	4	weak	weak	...	...	...	...	...	...
	5	1.26	0.103×10^4	4.5×10^{-3}	1.6	1.23×10^{-3}	2.81×10^{-3}	5.9	13.5
IGY-15	1		0.484×10^4		16.0				
	2		0.051×10^4		1.8				
	3		0.048×10^4		2.8				
	4		0.238×10^4		6.0				
IGY-18	1	3.79	0.180×10^4	17.7×10^{-3}	10.4	2.11×10^{-3}	1.70×10^{-3}	5.77	4.6
	2	4.16	0.222×10^4	8.0×10^{-3}	4.3	1.88×10^{-3}	1.86×10^{-3}	5.1	5.1
	3	2.83	0.229×10^4	12.4×10^{-3}	7.6	1.24×10^{-3}	1.63×10^{-3}	3.4	4.4
	4	1.88	0.133×10^4	6.0×10^{-3}	3.6	1.41×10^{-3}	1.67×10^{-3}	3.8	4.6
	5	2.05	0.126×10^4	6.0×10^{-3}	4.6	1.62×10^{-3}	1.30×10^{-3}	4.4	3.5
	6	2.59	0.167×10^4	9.6×10^{-3}	6.8	1.55×10^{-3}	1.41×10^{-3}	4.2	3.8
	7	3.72	0.245×10^4	13.0×10^{-3}	8.4	1.51×10^{-3}	1.55×10^{-3}	4.1	4.2
	8	5.90	0.402×10^4	12.5×10^{-3}	8.4	1.47×10^{-3}	1.49×10^{-3}	4.0	4.1
	9	4.70	0.410×10^4	10.3×10^{-3}	7.1	1.15×10^{-3}	1.45×10^{-3}	3.1	4.0
	10	2.18	0.317×10^4	4.9×10^{-3}	5.4	0.69×10^{-3}	0.91×10^{-3}	1.9	2.5
	11	3.99	0.491×10^4	4.2×10^{-3}	4.5	0.81×10^{-3}	0.93×10^{-3}	2.2	2.5
	12	74.6	5.860×10^4	107.2×10^{-3}	84.2	1.27×10^{-3}	1.27×10^{-3}	3.5	3.5
	13	3.88	0.283×10^4	13.0×10^{-3}	10.8	1.34×10^{-3}	1.20×10^{-3}	3.7	3.3
	14	1.71	0.184×10^4	6.9×10^{-3}	9.2	0.93×10^{-3}	0.75×10^{-3}	2.5	2.0
	15	3.95	0.410×10^4	10.0×10^{-3}	9.7	0.97×10^{-3}	1.03×10^{-3}	2.6	2.8
	16	3.17	0.426×10^4	3.2×10^{-3}	4.6	0.74×10^{-3}	0.70×10^{-3}	2.0	1.9
	17	4.84	0.174×10^4	4.8×10^{-3}	4.2	2.78×10^{-3}	1.14×10^{-3}	2.4	3.1
	18	2.22	-0.218×10^4	7.8×10^{-3}	...				
	19–20–21	1.71	0.089×10^4	3.4×10^{-3}	5.8	1.92×10^{-3}	3.02×10^{-3}	5.2	8.2
	22	1.60	0.084×10^4	2.4×10^{-3}	2.0	1.88×10^{-3}	1.06×10^{-3}	5.1	2.9
IGY-18 Photon counter	1		0.349×10^4		18.0			1.06	1.18
	2		0.475×10^4		6.8			0.98	1.32

above the balloon. These electrons may either be a part of the solar corpuscular stream generating the aurora when incident on the atmosphere or may be locally accelerated by the effects of this stream.

2. *Energy*.—From Table II and Fig. 2 we estimate 60 kev on IGY-3 and 100 kev on IGY-18. This energy is in terms of an ordinary tungsten target x-ray tube in which the given energy is the peak ac voltage applied to the tube. The apparent energy difference between IGY-3 and IGY-18 may possibly be attributed to the greater depth in the atmosphere of the balloon on IGY-18, and the consequent "hardening" of the x-ray spectrum. The energy estimate from the ratio single-counter/photon-counter on IGY-18 seems somewhat higher than from the ratio of ions/count, but because of the crudeness of the x-ray calibration this is not a contradiction.

As pointed out previously,[1] the sun-earth transit time of corpuscular streams of 20 to 48 hours represents a velocity of $0.01c$, or an electron energy of 30 ev. The observed time correlation of the x-rays with the aurora therefore implies an electron acceleration mechanism near the earth. For protons, however, the transit time is consistent with a considerably higher energy in the

TABLE II. Summary of auroral x-ray data.

Flight No., Date	Flight total Integrated intensity: Ion pairs in chamber	Flight total Integrated intensity: r units	Time of observation Hours	Peak intensity: ion pairs/sec in chamber	Peak intensity: mr/hr	Weighted mean X-ray ratio / Cosmic-ray ratio	Mean measured x-ray energy Kilovolts	Mass abs. coeff., μ, in the atmosphere cm²/g	Atmospheric depth g/cm²
IGY-3 June 30–July 1, 1957	1.96×10^{10}	3.12×10^{-5}	3.5	3.56×10^7	0.20	6.39	≈ 60	0.18	9.6
IGY-15 Sept. 12–13, 1957	...				Estimated >20 at 10 g/cm²	...	Consistent with 100 kev but not directly measured	0.15	47
IGY-18 Sept. 22–23, 1957 without peak 12	3.87×10^{10}		9.0	1.12×10^7		3.73	≈ 100	0.15	14
IGY-18, peak 12	4.73×10^{10}		0.67	6.80×10^7	0.39	3.46	≈ 100	0.15	14
IGY-18, total	8.60×10^{10}	1.37×10^{-4}	9.0						
IGY-18, photon counter						1.02	>100	<0.15	14

range 10–50 kev. This energy is also that observed directly by Meinel[6] in the Doppler-shifted H_α spectrum of auroral hydrogen. The acceleration process could therefore be of the type of an *exchange* of energy between protons and electrons in the solar stream, as suggested by Kellogg,[1,7] or between the protons in the stream and electrons in the high atmosphere.

3. Intensity.—The intensity fluctuates over wide limits within one storm. In Table II we list the integrated intensity for the period of the storm observed while the balloon was flying, in terms of total ion pairs in the chamber. This has been converted to roentgen units using the estimated energy. The conversion to r units is probably a low estimate as the x-rays are not monochromatic. The integrated intensity ranges from 0.03 to 0.14 mr. The peak intensity recorded so far is 0.4 mr/hr. (If the ion chamber is compared with a calibrated r meter on exposure to the lab x-ray machine, a factor of 10 greater dosage is obtained, which gives the value reported earlier.[1] This factor arises because of the stopping power of the 0.5-mm steel wall of the ion chamber.)

The peak rate measured on IGY-15 at 47 g/cm^2 maximum depth, when extrapolated back to 10 g/cm^2 using $\mu=0.15$ cm^2/g, gives a value of 4100 counts/sec, or 207 times the peak observed on IGY-3, and 49 times the peak observed on IGY-18. The intensity would thus be at least 20 mr/hr. An alternative possibility is that the energy observed on IGY-15 is much higher, with a correspondingly lower μ value. If one considers the "hardening" process in passage down through the atmosphere, however, one is forced again to the conclusion that the intensity at very high altitude must have been phenomenally high, and above the atmosphere may have exceeded 500 mr/hr for a period of at least 10 minutes.

The location of the balloon with respect to the specific auroral regions generating the x-rays certainly affects the observed intensity, and at present these details have not been completely investigated.

4. Estimate of electron current.—We assume that the x-rays are produced by electrons incident on the high atmosphere. These electrons are brought to rest by range absorption at considerable heights above the balloon. We assume that these electrons have an initial energy characteristic of the observed x-rays, and determined by the laboratory calibration of the ion chamber and counter. This lies between 50 and 100 kev. The energy spectrum of the incident electrons is unknown, but as the x-rays produced are characteristic of a thick air target, electrons of all energies will contribute to the x-ray flux in any case. This flux is attenuated by the atmosphere between the point of production and the balloon with a mass absorption coefficient depending on x-ray energy. This process "hardens" the x-rays. We shall ignore for the present the details of the production and attenuation process and compute the electron flux on the basis of the observed x-ray flux and characteristic energy observed at balloon heights. This will be a lower limit, as low-energy quanta produced in the bremsstrahlung process are undetected and ignored.

The electron current density is

$$J=[(dE/dx)_{\text{collision}}/(dE/dx)_{\text{radiation}}]\times 2(\text{x-ray energy flux})\times e/(\text{energy per electron}),\quad (1)$$

where e is the electron charge, and the factor *2* is due to the fact that half of the x-rays are lost upwards on the average. This assumes a uniform electron bombardment over a large area above the balloon, so that x-ray flux is constant with lateral direction. For the ratio of collision loss to radiation loss we use the relation given, for example, by Fermi[8]:

$$(dE/dx)_{\text{collision}}/(dE/dx)_{\text{radiation}}=800/Z\epsilon,\quad (2)$$

where Z=atomic number of stopping material and ϵ=energy of electrons in Mev. The x-ray energy flux passing through the ion chamber is

$$N=\lambda dN/dx,\quad (3)$$

where λ=absorption length in argon$=1/\mu$, and dN/dx =observed rate of energy loss in chamber, in ev/g sec, given by

$$\frac{dN}{dx}=\frac{i}{2}\left(\frac{w}{e}\right)\left(\frac{1}{m}\right),\quad (4)$$

where w=electron volts/ion pair, $m=\rho V$=mass of argon in ion chamber, and i=ion current. Finally,

$$J=\frac{800\lambda iw}{Z\epsilon^2\times 10^6}.\quad (5)$$

We use $\lambda=2.2$ g/cm^2 for 60-kev x-rays in argon,[9] $w=26$ ev/ion pair, $Z=7$ for air, $\epsilon^2=0.0036$ (Mev)^2, $m=123$ g argon, $i=22\times10^{-12}$ amp (peak current for burst 12, IGY-18), and $J=5\times10^{-13}$ amp/cm^2$=3\times10^6$ electrons/cm^2 sec$=5$ ma/km^2. The actual current density must be higher due to neglect of low-energy photons and the attenuation of the observed photons in the atmosphere above the balloon at a nominal depth of 10 g/cm^2. Furthermore, in Eq. (5) we use for ϵ the incident energy. The average energy during the absorption process must be lower, which increases the absorption/radiation ratio and the final computed electron current.

Chamberlain[10] and others have estimated the proton flux associated with the production of Doppler-shifted H_α in the spectra of strong aurorae at Yerkes Observa-

[6] A. B. Meinel, Astrophys. J. **113**, 50 (1951).
[7] Paul J. Kellogg, Phys. Rev. **108**, 1093 (1957).

[8] E. Fermi, *Nuclear Physics* (University of Chicago Press, Chicago, 1950), p. 47.
[9] A. H. Compton and S. K. Allison, *X-Rays in Theory and Experiment* (D. Van Nostrand Company, Inc., Princeton, New Jersey, 1935), p. 800.
[10] J. W. Chamberlain, Astrophys. J. **120**, 360 (1954).

tory at a latitude similar to Minneapolis and find 10^7-10^8 protons/cm^2 sec. If one considers our electron flux to be a low estimate, one may conclude that there is an electron component in auroral storms of the same order of intensity and equal in energy to the proton component. This is consistent with the electrical neutrality of the gas plasma entering the earth's magnetic field from the sun. The neutral character of the corpuscular stream has long been postulated to account for the presence of particles of magnetic rigidity far below the cutoff rigidity predicted by geomagnetic theory for the latitudes at which aurorae are observed. For example, the storm of September 22–23 was observed over Mexico City, at a geomagnetic latitude of 29° and a cutoff rigidity of 4 Bv.

Van Allen and co-workers,[11] using rocket-borne equipment, have reported many examples of high counting rates above the atmosphere and have interpreted them as auroral x-rays or, at very high altitudes, as the primary auroral electrons themselves. These observations are most frequent in the auroral zone, and for that reason the authors infer that the radiation is part of the aurora. The rocket counter did not show an increase below about 40 km. Van Allen concludes that the electron flux varies from 10^6-10^8 electrons/cm^2 sec, in very reasonable agreement with our measurements. The energies extend from 10–100 kev, lower in energy than the balloon energy range, which undoubtedly reflects the "hardening" with the greater atmospheric depth at which balloons float. The auroral storms observed at Minneapolis are furthermore sub-auroral belt phenomena representing a much higher intensity of disturbance, and possibly a higher average electron energy, than observed by Van Allen in the auroral zone. Since Flight IGY-18 on September 22, when we definitely established that our observations are not charged particles and are most probably x-rays, we believe that the phenomenon is basically of the same origin as the soft radiation observed by Van Allen.

Another observation of the soft radiation has been made by Anderson[12] on a balloon flight at approximately 10 g/cm^2 at Ft. Churchill in August, 1957. The balloon equipment was very similar to the Minnesota IGY apparatus. The observation was made in the daytime so that the auroral storm was not visible, but the presence of a magnetic storm and other evidence, including a cosmic-ray decrease associated with the storm, indicated the presence of a solar-produced corpuscular bombardment. Anderson reports that the photon nature of the disturbance was established by the increases observed in a single counter and ion chamber, but not observed in a coincidence telescope sensitive only to charged particles.

To account for the constant luminosity of auroral rays, which often extend above 300 km and encompass a density factor of 100 in the atmosphere, Chamberlain[13] has proposed a discharge theory of visible excitation. Assuming a constant electric field in the ray, the energy fed to the electrons at high altitude (where the mean free path is long) is high, and decreases for lower levels and smaller mean free paths. The density factor is thus compensated, and constant luminosity results. Chamberlain estimates the mean electron energy at the bottom of a ray (≈ 100 km) to be 0.32 ev and the flux 6×10^{12} electrons/cm^2 sec. The *power* in an auroral ray is thus about 3 kw/km^2. This power is of the same order of magnitude as that delivered by the x-ray electrons, or by the protons. This power seems also to be consistent with visual luminosity estimates by the Cornell group (private communication). One must therefore find a mechanism for feeding the available power from the incident particle stream into the ray discharge so as to give the effective constant electric field postulated by Chamberlain.

We are at present correlating the x-ray bursts measured during the three storms with geophysical data from many IGY observations and these results will be described in a separate communication.

In view of the great variability of the auroral phenomenon, one must hope for much better documentation of single auroral storms so that the visual forms, x-ray and visible spectral features, luminous intensities, and possibly local electric and magnetic fields may be accurately time-correlated. Such data would justify more exact computations of the type referred to and described above.

ACKNOWLEDGMENTS

The authors wish to acknowledge the major contribution of many members of the Physics Department staff for the instrumentation and operation of the IGY balloon program. The photon counter was designed and constructed by Mr. Dan McFadden. Frequent discussions with Professor Paul Kellogg concerning the magnetohydrodynamical problems in these phenomena have been very enlightening.

[11] J. A. Van Allen, Proc. Natl. Acad. Sci. U. S. **43**, 57 (1957).
[12] K. A. Anderson, Bull. Am. Phys. Soc. Ser. II, **2**, 349 (1957).
[13] J. W. Chamberlain, *Belfast Symposium on the Aurora and Airglow* (Pergamon Press, London, 1955).